ELSEVIER

Carbohydrate Research 304 (1997) 219–228

CARBOHYDRATE RESEARCH

Solution conformation and dynamics of an extracellular polysaccharide isolated from *Bradyrhyzobium* as deduced from ^{1}H-NMR off resonance ROESY and ^{13}C-NMR relaxation measurements

Ana Poveda [a], Mónica Santamaría [b], Manuel Bernabé [c], Alfonso Rivera [d], Javier Corzo [b], Jesús Jiménez-Barbero [c,*]

[a] *Servicio Interdepartamental de Investigación, Universidad Autonoma de Madrid, Cantoblanco 28049 Madrid, Spain*

[b] *Departamento de Bioquímica y Biología Molecular, Universidad de la Laguna, 38071 Tenerife, Spain*

[c] *Instituto Quimica Organica, CSIC, Juan de la Cierva 3, 28006 Madrid, Spain*

[d] *Centro de Investigacion Basica, Smith Kline Beecham, Tres Cantos, Madrid, Spain*

Received 31 March 1997; accepted 23 July 1997

Abstract

The conformational and dynamical features of an extracellular branched deacetylated polysaccharide isolated from *Bradyrhizobium* (*Chamaecytisus proliferus*) have been investigated by homo and heteronuclear NMR methods. ^{1}H-NMR cross relaxation rates have been obtained for this polysaccharide through regular NOESY and ROESY spectra as well as by modern off resonance ROESY techniques. Local proton–proton correlation times as well as interproton distances have been obtained. ^{13}C-NMR relaxation parameters (T_1, T_2, NOE) have also been measured at two different magnetic fields and interpreted using different approximations based on the Lipari and Szabo model free approach. The analysis of the data indicates the existence of important flexibility for the different linkages of the polysaccharide. Motions in the range of several ns contribute to the relaxation of the macromolecule, although faster internal motions in the 600–800 ps timescales are also present. These time scales indicate that segmental motions as well as internal motions around the glycosidic linkages are the major sources of relaxation for this molecule at 299 K.

Keywords: NMR; Relaxation; Dynamics; Off resonance ROESY; Model free approach

* Corresponding author. Fax: +34-1-5644853; e-mail iqojj01@pinar1.csic.es.

0008-6215/97/$17.00
PII S0008-6215(97)00238-3

1. Introduction

Knowledge of the three dimensional structure of oligosaccharide and polysaccharide molecules is of paramount importance to explain the recognition processes in which they are involved [1]. In addition, the existence of rigid or flexible structures is of prime importance in recognition phenomena, since any bimolecular binding process is, in principle, entropically unfavourable due to the formation of a single molecule of complex [2]. The acidic polysaccharide produced by *Bradyrhizobium* (*Chamaecytisus proliferus*) is probably involved in the symbiotic process, due to its specific binding with plant lectins [3]. The structure and overall conformational features of this polysaccharide has been deduced by us in the previous paper [4]. The deacetylated polysaccharide has the following sequence → 3)-[α-D-Gal*p*-(1 → 6)]-α-D-Glc*p*-(1 → 3)-β-D-Glc*p*-(1 → 3)-α-D-Gal*p*A-(1 → 3)-α-D-Man*p*-(1 → .

This primary structure is particularly interesting from the conformational point of view, since it consists of a variety of α and β linkages, which may give particular conformational and dynamical properties to the polysaccharide [5].

The extent and nature of the motion around the glycosidic linkages of oligosaccharides remains an open question [6], and even detailed analysis of experimental and theoretical results have concluded either constrained conformations [7] or conformational averaging [8] for carbohydrate structures. In addition, recent investigations have established that the rates of overall and internal motions of small and medium-size oligosaccharides may occur on similar timescales [9,10]. Thus, indications of internal motions around the glycosidic linkages of different disaccharides [11] and larger oligosaccharides have been obtained using both homo and heteronuclear NMR spectroscopy, as also employed for other biomolecules [12–14]. In this context, we decided to study the conformation and dynamic features of this polysaccharide [15], since, in principle, and due to its size, the time scales of the overall tumbling and of the internal motions around the glycosidic linkages should be fairly different and permit the analysis of the dynamical properties of the different glycosidic linkages. In addition, we have tried to characterise the extent of restriction to motion around the different α- and β-(1 → 3) linkages of this molecule, with particular emphasis to the branching point [4]. Measurements of heteronuclear relaxation parameters for polysaccharides have allowed variations of the relative motion of side chain versus backbone residues in branched polysaccharides to be probed [15,16]. Nevertheless, a detailed and quantitative solution to the problem of polysaccharide dynamics is far from trivial and different dynamic models have been developed to describe the motion of these biomolecules. We now report on the application of NMR relaxation parameters [17] to characterise the motional properties of the polysaccharide. It seems necessary to consider that, for flexible polysaccharides, above a given molecular weight, it has been reported that relaxation parameters are independent of chain length, because of the dominant contribution of segmental motion to the spectral density function [18]. Our relaxation data have been interpreted by using the model free approach proposed by Lipari and Szabo [19], since in principle, this model is useful to characterise the molecular dynamics of flexible macromolecules, as the polysaccharide presented herein. In addition, different approximations of this model free approach have been employed [20,21] (see also Experimental), in an attempt to obtain information on the reorientation correlation times as well as on the local dynamics at the glycosidic linkages [22,23].

2. Experimental

Molecular mechanics and dynamics calculations.—Molecular mechanics and dynamics calculations have been described in a separate paper [4].

NMR spectroscopy.—NMR experiments were recorded on JEOL 400 and Varian Unity 500 spectrometers, using an approximately 15 mg/mL solution of the polysaccharide. No attempts were made to use other concentrations to evaluate the influence of this parameter in the resulting data.

^{1}H-NMR experiments.—Selective inversion of the anomeric protons was performed using the DANTE-Z module [22] during 60 ms. 1D-NOESY experiments were recorded using mixing times of 100, 200, 300, and 400 ms. ROESY experiments [23] used mixing times of 100, 200, 300, and 400 ms. The *rf* carrier frequency was set at δ 6.0 ppm, and the spin locking field was 2.5 KHz. Good linearity of the build up curves was observed up to 250 ms (NOESY) and 300 ms (ROESY). Estimated errors are smaller than 10%. Assuming that the motion of two interacting protons can be described by a monoexponential autocorrelation function, the corresponding cross relaxation rates are:

$$\sigma_{NOESY} = (k^2/10r^6)[6J(2\omega) - J(0)] \quad (1)$$

$$\sigma_{ROESY} = (k^2/10r^6)[2J(0) + 3J(\omega)] \quad (2)$$

Off resonance ROESY experiments, using a trapezoidal adiabatic pulse as described [24–26] were also performed using mixing times of 50, 100, 150, 200, 250, and 300 ms. Cross relaxation rates were estimated from the build up courses by extrapolation at zero mixing time [27,28]. The spin locking carrier frequency was positioned at 22 different offsets in order to estimate the longitudinal and transversal cross relaxation rates, σ_{NOESY} and σ_{ROESY}. The theory under off resonance ROESY has been detailed [24–26]. However, a brief introduction will be given here for sake of clarity.

The off resonance adiabatic pulse locks the spins along the effective field, which makes a ϕ angle with the z axis. Thus, tilting angles ϕ between 0 and ± 55 degrees were employed.

The tilting angle is defined as follows:

$$\phi = \arctan(\omega_1/\omega_{offset}) \quad (3)$$

The spin locking field was 8.8 KHz. The experiments were carried out at 298 K. Cross relaxation rates were obtained from off-resonance ROESY measurements as described from the dependence of the NOE cross peak intensities versus the tilted angle, according to the following expressions:

$$\sigma_{obs} = \sigma_{NOESY} \cos^2\phi + \sigma_{ROESY} \sin^2\phi \quad (4)$$

$$\rho_{obs} = \rho_{NOESY} \cos^2\phi + \rho_{ROESY} \sin^2\phi \quad (5)$$

Effective correlation times and thus, interproton distances, for selected proton pairs may be obtained from $\sigma_{NOESY}/\sigma_{ROESY}$ ratios, since they only depend on τ_c. Developing the spectral density functions, $J(n\omega)$, in function of the correlation time, τ_c, and of the spectrometer frequency, ω_0.

$$\sigma_{ROESY}/\sigma_{NOESY} = (5 + 22\omega_0^2\tau_c^2 + 8\omega_0^4\tau_c^4) / (5 + \omega_0^2\tau_c^2 - 4\omega_0^2\tau_c^4) \quad (6)$$

which is a quartic equation in τ_c, which can be easily solved. It should be stressed that the assumption made here does not require equal mobility between different proton pairs, as in a rigid molecule. Therefore, it is possible to obtain internuclear distances r (geometrical parameter) and local correlation times (dynamic parameter) for any pair of protons. This approach reduces the intrinsic error resulting from the use of an internal reference (as in the isolated spin pair approximation).

^{13}C - NMR experiments.—T_1 relaxation times at 100 and 125 MHz were obtained by using the regular 1D-inversion recovery at 298 K. At least six different relaxation delays were used in every experiment. Heteronuclear NOEs were obtained by comparing the intensities of the signals of two spectra acquired by the standard 1D-protocol [27]. T_2 transverse relaxation times were obtained by the CPMG pulse sequence [17]a. In all cases, the given values are averaged among the different measurements performed. Estimated errors are in all cases smaller than 10%.

$$T_1^{-1} = (\Omega/20)[J(\omega_H - \omega_C) + 3J(\omega_C) + 6J(\omega_H + \omega_C)] \quad (7)$$

$$T_2^{-1} = (\Omega/20)[4J(0) + J(\omega_H - \omega_C) + 3J(\omega_C) + 6J(\omega_H) + 6J(\omega_H + \omega_C)] \quad (8)$$

$$\Omega = N\left(\frac{\gamma_C\gamma_H h}{2\pi r_{CH}^3}\right)^2 \quad (9)$$

$$NOE = 1 + \frac{\gamma_H}{\gamma_C} \times \frac{6J(\omega_C + \omega_H) - J(\omega_C - \omega_H)}{J(\omega_H - \omega_C) + 3J(\omega_C) + 6J(\omega_C + \omega_H)} \quad (10)$$

Fitting of the heteronuclear relaxation data.—The following models were employed:

Model I. The regular isotropic Lipari–Szabo model free approach [19], where τ_e represent a single effective correlation time describing the internal motions.

$$J(\omega) = \frac{S^2\tau_0}{(1 + \omega^2\tau_0^2)} + \frac{(1 - S^2)\tau}{(1 + \omega^2\tau^2)} \quad (11)$$

$$\tau = \tau_0\tau_e/(\tau_0 + \tau_e) \quad (12)$$

Model II. Extended isotropic Lipari–Szabo model free approach as described by Clore et al. [21]. Two different internal motions are considered, characterised by fast, τ_f', and slow, τ_s', correlation times. Order parameters for the corresponding motions are also included in the analysis.

$$J(\omega) = \frac{S^2\tau_0}{1 + (\omega\tau_0)^2} + \frac{(1 - S_f^2)\tau_f'}{1 + (\omega\tau_f')^2} + \frac{(S_f^2 - S^2)\tau_s'}{1 + (\omega\tau_s')^2} \quad (13)$$

$$S^2 = S_f^2 S_s^2 \quad (14)$$

$$\tau_i' = \tau_i\tau_0/(\tau_0 + \tau_i), \quad i = f, s \quad (15)$$

Model III. If τ_f is much smaller than τ_s, then the spectral density function simplifies to the following

$$J(\omega) = \frac{S^2\tau_0}{1+(\omega\tau_0)^2} + \frac{(S_f^2 - S^2)\tau_s'}{1+(\omega\tau_s')^2} \quad (16)$$

$$S^2 = S_f^2 S_s^2 \quad (17)$$

$$\tau_s' = \tau_s\tau_0/(\tau_0 + \tau_s) \quad (18)$$

Model IV. Symmetric top within the Lipari Szabo approach. In this case, for an anisotropically tumbling molecule, two correlation times are defined, $\tau_\perp$ and $\tau_\parallel$, along the short and long axis of the proellipsoid [19,20]. In addition, θ is the angle between the C–H relaxation vector and the symmetry axis.

$$J(\omega) = S^2 J_{anisot}(\omega) + (1 - S^2)\frac{\tau}{1+(\omega\tau)^2} \quad (19)$$

$$\tau^{-1} = \tau_0^{-1} + \tau_e^{-1} \quad (20)$$

$$J_{anisot}(\omega) = \frac{0.25(3\cos^2\theta - 1)^2\tau_a}{1+(\omega\tau_a)^2} + \frac{3\sin^2\theta\cos^2\theta)\tau_b}{1+(\omega\tau_b)^2} + \frac{0.75(\sin^4\theta)\tau_c}{1+(\omega\tau_c)^2} \quad (21)$$

Where:

$$\tau_a = \tau_\perp \quad (22)$$

$$(1/\tau_b) = 5/(6\tau_\perp) + 1/(6\tau_\parallel) \quad (23)$$

$$(1/\tau_c) = 1/(3\tau_\perp) + 2/(3\tau_\parallel) \quad (24)$$

For the heteronuclear relaxation parameters, a similar target function, *Rw*, was also defined:

$$Rw = \left(\sum_{i=1}^{n} \left[\left(T_{1i}^{calc} - T_{1i}^{exp}\right)^2 + \left(T_{2i}^{calc} - T_{2i}^{exp}\right)^2 + \left(NOE_i^{calc} - NOE_i^{exp}\right)^2 \right] \times \left[\left(T_{1i}^{exp}\right)^2 + \left(T_{2i}^{exp}\right)^2 + \left(NOE_i^{exp}\right)^2 \right]^{-1} \right)^{1/2} \quad (25)$$

with $Rw = 0$, for an exact fit. The subscript i represent data for a particular carbon atom, and n is the total number of carbons with available experimental data.

As stated above, either all the relaxation parameters or combinations of two of them were used. The parameter which was not taken into account in the fitting procedure, was employed as test of the goodness of the fitting approach. In all cases, for the different models, only the results of the best fitting (smallest *Rw*), that include all the experimental data are given in the text.

An estimation of the errors in the motional parameters obtained within each optimization was accomplished by fixing the maximum precision of the *Rw* in 0.001 around the best fitting value, and then observing the range of variability of the motional parameters. The minimization of the target functions *Rw* (homonuclear and heteronuclear) in the different calculations was accomplished, in an iterative way, by using a simplex-based algorithm [29] [1]. Since different variables had to be optimised, a recursive method was adopted, starting from 1, 2, up to a maximum of 5 (models II and IV) variables evaluated simultaneously. Different intervals of values of the variables were screened in order to find the global minimum.

3. Results and discussion

Molecular dynamics.—The study of the accessible amount of conformational space for the glycosic linkages of the polysaccharide was obtained through MD simulations, and has been described in detailed in the accompanying paper [4]. The obtained results indicated that, as least for this particular case, unrestrained MD simulations [4] provide a fair description of the motion around the different glycosidic linkages of this molecule. The polysaccharide may adopt a variety of three dimensional shapes.

^{1}H-NMR data.—The pyranoid rings (Fig. 1) can be described as essentially monoconformational: $^4C_1$, as deduced from the vicinal proton–proton couplings (data not shown). ^{1}H-NMR cross relaxation rates [27] (σ_{ROESY}, and σ_{NOESY}) were obtained from 1D-NOESY, 1D-ROESY, and 1D-off resonance ROESY (Fig. 2) measurements, after selective inversion of the anomeric protons. 2D-NOESY and 2D-ROESY experiments were also performed. At 298 K, NOESY peaks are negative at 500 MHz (Table 1). The presence of distinct internal motion for the different glycosidic linkages which constitute the polysaccharide was performed by obtaining $\sigma_{ROESY}/\sigma_{NOESY}$ ratios [24,26,30,31]. Provided that the motion is far from the extreme narrowing limit or the slow motion

[1] All programs in Pascal and source codes are available from the authors upon request.

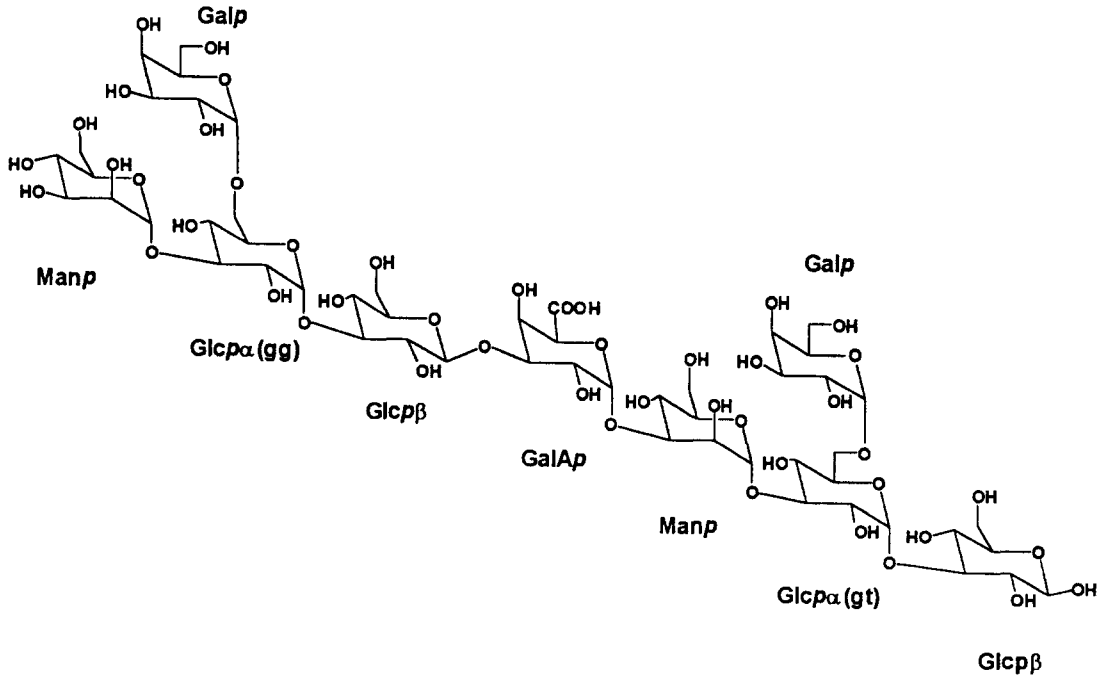

Fig. 1. Schematic view of the polysaccharide chain, showing the different residues.

regimes, all these ratios are independent of interproton distances and allow to estimate specific correlation times (see Experimental). The results are also given in Table 1. It can be observed that, within experimental error, there are relevant differences between the correlation times [6,9,10] obtained for the proton pairs of the different pyranoid rings (Table 2). The higher values are observed for residue A (α-Glc) and the lowest for residue D (α-Gal). The τ_c obtained for the other residues are in between. These are not unexpected results, since A is the only branched moiety, and residue D should experience both the motion around the main chain as well as additional fluctuations due to the motion of the (1 → 6)-chain [15,16]. Therefore, according to our results and as also described by other authors, the use of different local correlation times for the different proton pairs of oligosaccharide molecules is advisable.

Average interproton distances were estimated from the obtained effective τ_c and the experimental cross relaxation rates. A check of the internal consistency of the results was performed by back calculating the intraresidue proton–proton distances (Table 1). It can be observed that there is a fair agreement between experimental and modeled distances. Experimental interresidue distances were also calculated and then compared to those derived from the MD simulations (Table 1, see also Ref. [4] indicating that a satisfactory agreement was found between both sets of values. Overall correlation times around 2–5 ns are obtained. The physical meaning of the obtained correlation times is not evident, since overall reorientation, segmental, internal motions of the pendant groups, and librations of the pyranoid rings are independent sources of modulation of dipole–dipole interactions [15,32]. Nevertheless, the relatively small size of the obtained effective or overall correlation times by using these isotropic models (τ_c around 2–5 ns) indicates that local and segmental motions are the major sources of relaxation in this flexible polysaccharide [15,18]. The obtained values of the relaxation parameters could correspond to those of the segment similar in size to the critical molecular weight or degree of polymerisation for which relaxation parameters are independent of chain length [33]. In other flexible polysaccharides, the minimum oligomer size for which segmental motion dominates the spectral power density is between 10 and 15 monosaccharide units [15,18].

Two recent papers on the conformation and dynamics of oligosaccharides have also addressed the use of local correlation times to derive interproton distances, by simultaneous determination of the dipolar longitudinal and transversal cross relaxation rates through off-resonance ROESY measurements [25,26]. These authors also concluded that, for each pair of protons, a different correlation time should be used [17].

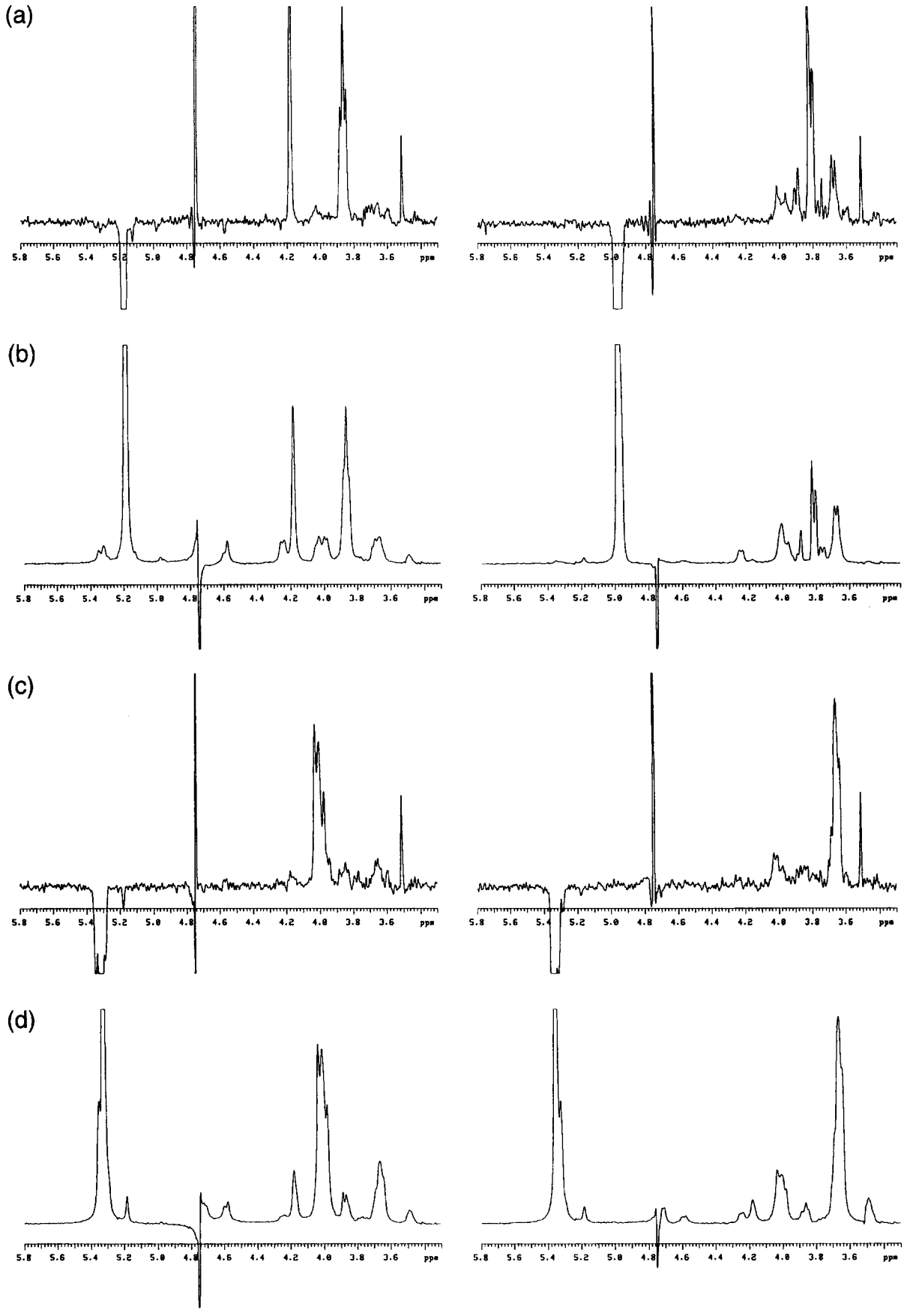
(a)
(b)
(c)
(d)
5.8 5.6 5.4 5.2 5.0 4.8 4.6 4.4 4.2 4.0 3.8 3.6 ppm

Table 1
σ_{NOE} and σ_{ROE} cross relaxation rates (s^{-1}) of the relevant intra and interresidue proton pairs of the polysaccharide isolated from *Bradyrhizobium* estimated from off resonance ROESY measurements

Proton pair	σ_{NOE}	σ_{ROE}	τ_{local}	Distance (Å)
H-1 A/ H-2 A	−1.18(0.02)	2.38(0.15)	5.5	2.54
H-1 A/ H-3 F	−1.18(0.02)	2.38(0.15)	5.5	2.54
H-1 B/ H-2 B	−1.37(0.03)	2.78(0.17)	4.6	2.39
H-1 B/ H-3 C	−1.17(0.02)	2.20(0.13)	3.6	2.40
H-1 C/ H-2 C	−1.30(0.03)	2.67(0.16)	3.8	2.33
H-1 C/ H-3 A	−1.39(0.03)	2.84(0.17)	4.0	2.34
H-1 D/ H-2 D	−1.31(0.03)	2.70(0.19)	3.3	2.28
H-1 D/ H-6a A	−0.16(0.01)	0.37(0.03)	1.6	2.82
H-1 D/ H-6b A	−0.21(0.01)	0.46(0.03)	1.7	2.77
H-1 F/ H-3 B	−1.30(0.03)	2.65(0.19)	5.1	2.46
H-1 F/ H-3 F	−1.31(0.03)	2.64(0.19)	5.4	2.48

Standard deviations are given between brackets. The corresponding local correlation times (ns) and interproton distances, using a $\langle r^{-6} \rangle^{-1/6}$ average, are also given. H-2A and H-3F show overlap.

Next, in order to try to characterise more profoundly the dynamic features of the polysaccharide, heteronuclear relaxation parameters were also measured.

^{13}C-NMR data.—Heteronuclear relaxation data are of paramount importance to detect the presence of internal motion in biomolecules, in general, [34] and in carbohydrates, in particular [10,11,15,17,35]. Regarding polysaccharides, relaxation parameters have been used either qualitative or quantitatively to deduce their dynamical features [15–18]. Thus, in this case, T_1 and T_2 relaxation times and heteronuclear NOEs [17,34] of several ^{13}C sites were obtained at 100 and 125 MHz. Inspection of the average values (Table 3) of T_1 for the different residues of the polysaccharide seems to indicate that the α-Galp-(1 → 6)-linked ring (with larger T_1 and NOEs) is less constrained than the α-and β-linked (1 → 3)-residues (smaller T_1 and NOEs). A similar trend has been previously observed in branched dextrans and, indeed, those values were used to assign the different anomeric carbon atoms of a series of polysaccharides in terms of branched, side chain, and non substituted residues [15–18]. The model free approach was employed for the analysis of the relaxation data, since, in principle, it is adequate for flexible macromolecules. First, an isotropic model was employed. The Lipari and Szabo analysis [10,17,19,20] of the heteronuclear data (Table 2) allowed to estimate an overall correlation time of ca. 5 ns, with short local correlation times, τ_e, smaller than 500 ps for all the glycosidic linkages. The values obtained are fairly similar to those obtained from the homonuclear data. S^2 values for the methine carbons are between 0.6 and 0.8 units. The sizes of the overall correlation time (around 5 ns) indicate that local and segmental motions are the major sources of relaxation of this polysaccharide [15,33].

Nevertheless, this isotropic analysis did not match the T_2 values in a satisfactory way, since the expected values were significantly higher than those experimentally measured [15,17]. Thus, in a second step, and considering that different motions contribute to the relaxation parameters, an extended Lipari–Szabo model was applied, as proposed by Clore and coworkers [21] (see Experimental). In this model, two different internal motion correlation times and order parameters are considered, accounting for the existence of very fast (τ_f) and moderately fast (τ_s) internal motions. If τ_f is at least one order of magnitude smaller than τ_s, a truncated form may be considered (models II and III, respectively). Both models

Fig. 2. (a) 1D-NOESY (bottom right), 1D-ROESY (top right) spectra obtained after inversion of the anomeric proton of residue A at 299 K. In all cases, mixing time is 100 ms. (b) 1D-NOESY (bottom left), 1D-ROESY (top left) spectra obtained after inversion of the anomeric proton of residue B at 299 K. (c) 1D-NOESY (bottom left), 1D-ROESY (top left) spectra obtained after inversion of the anomeric proton of residue C at 299 K. (d) 1D-NOESY (bottom right), 1D-ROESY (top right) spectra obtained after inversion of the anomeric proton of residue D at 299 K.

Table 2
Average motional parameters of the methine carbon–proton vectors of the different pyranoid rings from ^{13}C-NMR relaxation data obtained for the polysaccharide isolated from *Bradyrhizobium* using Model I, $\tau_0 = 5727 \pm 90$ ps, $Rw = 0.033$

Residue	τ_c (ps)	S^2	Carbon atom	τ_c (ps)	S^2
α-Glc*p*	560	0.72	α-GalA *p*	510	0.67
α-Man*p*	430	0.68	α-Gal*p*	360	0.65
β-Glc*p*	550	0.66			

Table 5
Average motional parameters of the methine carbon–proton vectors of the different pyranoid rings from ^{13}C-NMR relaxation data obtained for the polysaccharide isolated from *Bradyrhizobium* using Model III, $\tau_0 = 11984 \pm 400$ ps, $Rw = 0.006$

Residue	τ_s' (ps)	S_s^2	S_f^2	Residue	τ_s' (ps)	S_s^2	S_f^2
α-Glc*p*	840	0.39	0.96	α-GalA *p*	695	0.83	0.76
α-Man*p*	650	0.38	0.78	α-Gal*p*	580	0.77	0.69
β-Glc*p*	735	0.38	0.89				

(Tables 4 and 5) provided a fairly satisfactory matching between expected and observed data. Overall correlation times are higher than 10 or 20 ns, depending on the consideration of either the truncated or the extended model, respectively, while the slow internal motions are between 600 and 800 ps (extended model). Finally, the very fast internal motions (model IV) are smaller than 100 ps. Regarding order parameters, the branched A rings present the largest restriction to motion, while the Gal side chains show the smallest S^2. It seems that the obtained overall correlation times may correspond to the segmental and global motion timescale, while the fast correlation times probably include the motion around the ω torsions, around the Φ/Ψ glycosidic linkages, and the librations of the pyranoid rings [32].

Finally, in order to explore the possibility of the existence of anisotropic motion, the polysaccharide was considered as a symmetric top molecule [20], characterised by two different overall correlation times, $\tau_\perp$ and $\tau_\parallel$, and a term that include local motion correlation time, τ. Although the election of any model for a polysaccharide entity maybe a matter of discussion [15–18], the fitting of the data showed that the existence of a proellipsoid shape could be possible. In fact, there is again a satisfactory matching between all the experimental and expected relaxation data (Table 6). The ratio between $\tau_\perp/\tau_\parallel$ is about 50, $\tau_\parallel$ being around 0.5 ns. The internal motion correlation times are again of a few tens of ps. This anisotropic analysis of the data also allowed to conclude that the outer ring displays rather significant local motion. Similar heteronuclear relaxation analysis have been recently performed for other polysaccharides [10,20,36–38]. For heparin-related polysaccharides [10,20,36], the experimental values have been explained assuming anisotropy of motion following a symmetric top model. On the other hand, Brisson et al. have demonstrated [37] that the type III group B *Streptococcus* capsular polysaccharide un-

Table 3
Average longitudinal relaxation times (s), heteronuclear NOEs and transversal relaxation times (s) for the different pyranoid rings of the polysaccharide isolated from *Bradyrhizobium* at 100 and 125 MHz and 299 K

Residue	T_1 100 MHz	T_1 125 MHz	NOE 100 MHz	NOE 125 MHz	T_2 100 MHz	T_2 125 MHz
α-Glc*p*	0.28	0.32	1.49	1.40	0.046	0.050
α-Man*p*	0.35	0.42	1.64	1.52	0.058	0.061
β-Glc*p*	0.31	0.36	1.56	1.45	0.050	0.053
α-GalA *p*	0.33	0.40	1.61	1.49	0.054	0.057
α-Gal*p*	0.38	0.45	1.73	1.61	0.060	0.062

Experimental errors are smaller than 10%.

Table 4
Average motional parameters of the methine carbon–proton vectors of the different pyranoid rings from ^{13}C-NMR relaxation data obtained for the polysaccharide isolated from *Bradyrhizobium* using model II, $\tau_0 = 24733 \pm 2830$ ps, $Rw = 0.004$

Residue	τ_s' (ps)	τ_f' (ps)	S_s^2	S_f^2	Residue	τ_s' (ps)	τ_f' (ps)	S_s^2	S_f^2
α-Glc*p*	970	20	0.21	0.80	α-GalA *p*	790	10	0.20	0.68
α-Man*p*	755	13	0.21	0.64	α-Gal*p*	704	18	0.22	0.61
β-Glc*p*	850	11	0.20	0.73					

Table 6
Motional parameters from ^{13}C-NMR relaxation data of the methine carbon–proton vectors of the different pyranoid rings obtained for the polysaccharide isolated from *Bradyrhizobium* using model IV, $\tau_{\perp} = 24{,}200 \pm 2500$ ps, $\tau_{\parallel} = 523 \pm 25$ ps, $Rw = 0.008$

Residue	θ	τ (ps)	S^2	Residue	θ	τ (ps)	S^2
α-Glc*p*	73	10	0.84	α-GalA *p*	86	16	0.71
α-Man*p*	85	16	0.64	α-Gal*p*	87	30	0.59
β-Glc*p*	82	15	0.77				

dergoes helical formation. Isotropic motion may be assumed, although different mobilities for the backbone and the side chains are observed. Xu and Bush [38] have implicated the superimposition of substantially different internal motion timescales to explain the relaxation data of the cell wall polysaccharide of *Streptococcus mitis* J22. Given the flexibility of the polysaccharide described herein, the latter interpretation seems to be more reasonable from the physical point of view.

In any case, independently of the model, the results indicate that the relaxation of the D/E ring atoms is modulated by the motion of the linear chain as well as by that existing around its glycosidic linkage. For the main chain, the data again indicate the existence of a higher restriction to fast motions for the branched Glc*p* residue.

In conclusion, the homonuclear relaxation data have provided evidence of the importance of internal and segmental motions in this polysaccharide. Heteronuclear parameters have permitted to detect that motions in different timescales are able to produce dipole–dipole relaxation in this polysaccharide. The nature of these motions are probably related to segmental motion and to reorientation around the hydroxymethyl and glycosidic torsion angles. Both the extended Lipari–Szabo approach [21] and an anisotropic symmetric top model provide a satisfactory agreement between expected and observed data. Giving the flexibility of the polysaccharide, the first model seems to be more realistic.

Acknowledgements

Financial support of DGICYT (project PB93-0172) is gratefully acknowledged. We thank Prof. Martín-Lomas for his interest and the SIdI-UAM for the facilities provided throughout this work. The work of M.S. and J.C. was supported by a grant of the Canary Islands Government.

References

[1] T. Peters and B.M. Pinto, *Curr. Opin. Struct. Biol.*, 6 (1996) 655–663.
[2] M.S. Searle and D.H. Williams, *J. Am. Chem. Soc.*, 114 (1992) 10,690–10,697.
[3] J. Corzo, M. Leon-Barrios, V. Hernando-Rico, and A.M. Gutierrez-Navarro, *Appl. Environ. Microbiol.*, 60 (1994) 4531–4536.
[4] A. Poveda, M. Santamaría, M. Bernabé, A. Prieto, M. Bruix, J. Corzo, and J. Jiménez-Barbero, *Carbohydr. Res.*, 304 (1997) 209–217.
[5] H. van Halbeek, *Curr. Opin. Struct. Biol.*, 4 (1994) 697–709.
[6] (a) M. Hricovini, R.N. Shah, and J.P. Carver, *Biochemistry*, 31 (1992) 10,018–10,023; (b) T.J. Rutherford, J. Partridge, C.T. Weller, and S.W. Homans, *Biochemistry*, 32 (1993) 12,715–12,724; (c) C.A. Bush, *Curr. Opin. Struct. Biol.*, 2 (1992) 655–663; (d) K.G. Rice, P. Wu, L. Brand, and Y.C. Lee, *Curr. Opin. Struct. Biol.*, 3 (1993) 669–674.
[7] (a) C. Mukhopadhyay, K.E. Miller, and C.A. Bush, *Biopolymers*, 34 (1994) 21–29; (b) T.J. Rutherford, D.G. Spackman, P.J. Simpson, and S.W. Homans, *Glycobiology*, 4 (1994) 59–68; (c) R.U. Lemieux, *Chem. Soc. Rev.*, 18 (1989) 347–374; (d) K. Bock, *Pure Appl. Chem.*, 55 (1983) 605–622.
[8] (a) J.P. Carver, *Pure Appl. Chem.*, 65 (1993) 763–770; (b) A. Ejchart, J. Dabrowski, and C.W. von der Lieth, *Magn. Res. Chem.*, 30 (1992) S105–S114; (c) T. Peters and T. Weimar, *J. Biomol. NMR*, 4 (1994) 97–116.
[9] L. Poppe and H. van Halbeek, *J. Am. Chem. Soc.*, 114 (1992) 1092–1094.
[10] (a) M. Hricovini and G. Torri, *Carbohydr. Res.*, 268 (1995) 159–175; (b) B.J. Hardy, W. Egan, and G. Widmalm, *Int. J. Biol. Macromol.*, 17–18 (1995) 149–160.
[11] (a) C. Meyer, S. Perez, C. Herve du Penhoat, and V. Michon, *J. Am. Chem. Soc.*, 115 (1993) 10,300–10,310; (b) I. Braccini, V. Michon, C. Herve du Penhoat, A. Imberty, and S. Perez, *Int. J. Biol. Macromol.*, 15 (1993) 52–55; (c) A. Poveda, J.L. Asensio, M. Martin-Pastor, and J. Jimenez-Barbero, *Chem. Comm.*, (1996) 421–422; (d) S. Bagley, H. Kovacs, J. Kowalewski, and G. Widmalm, *Magn. Reson. Chem.*, 30 (1992) 733–739; (e) L. Maler, J. Lang, G. Widmalm, and J. Kowalewski, *Magn. Reson. Chem.*, 33 (1995) 541–548; (f) J.F. Espinosa, J.L. Asensio, M. Bruix, and J. Jimenez-Barbero, *J. An. Quim. Int. Ed.*, 96 (1996) 320–324.
[12] R. Bruschweiler, B. Roux, M. Blackledge, C. Griesinger, M. Karplus, and R.R. Ernst, *J. Am. Chem. Soc.*, 114 (1992) 2289–2302.
[13] M. Philippopoulos and C. Lim, *J. Phys. Chem.*, 98 (1994) 8264–8273.
[14] R. Abseher, S. Ludemann, H. Schreiber, and O. Steinhauser, *J. Am. Chem. Soc.*, 116 (1994) 4006–4018.
[15] P. Dais, *Adv. Carbohydr. Chem. Biochem.*, 51 (1995) 63–161.

[16] F.R. Seymour and R.D. Knapp, *Carbohydr. Res.*, 81 (1980) 67–103.
[17] (a) J. Kowalewski and G. Widmalm, *J. Phys. Chem.*, 98 (1994) 28–34; (b) J.P.M. Lommerse, L.M.J. Kroon-Batenburg, J. Kron, J.P. Kamerling, and J.F.G. Vliegenthart, *J. Biomol. NMR*, 5 (1995) 79–94; (c) L. Maler, G. Widmalm, and J. Kowalewski, *J. Biomol. NMR*, 7 (1996) 1–7; (d) R. Roy, D. Tropper, A.J. Williams, and J.R. Brisson, *Can. J. Chem.*, 71 (1993) 1995–2006.
[18] (a) A.J. Benesi and D.A. Brant, *Macromolecules*, 18 (1985) 1109–1116; (b) D.A. Brant, H.S. Liu, and Z.S. Zhu, *Carbohydr. Res.*, 278 (1995) 11–26.
[19] G. Lipari and A. Szabo, *J. Am. Chem. Soc.*, 104 (1982) 4546–4559.
[20] M. Hricovini, M. Guerrini, G. Torri, S. Piani, and F. Ungarelli, *Carbohydr. Res.*, 277 (1995) 11–23.
[21] G.M. Clore, P.C. Driscoll, P.T. Wingfield, and A.M. Gronenborn, *J. Am. Chem. Soc.*, 29 (1990) 7387–7400.
[22] D. Boudot, D. Canet, J. Brondeau, and J.C. Boubel, *J. Magn. Reson.*, 83 (1989) 428–434.
[23] A.A. Bothner-By, R.L. Stephens, J.M. Lee, C.D. Warren, and R.W. Jeanloz, *J. Am. Chem. Soc.*, 106 (1984) 811–813.
[24] H. Desvaux, P. Berthault, N. Bilirakis, and M. Goldman, *J. Magn. Reson. A*, 108 (1994) 219.
[25] G. Lippens, J.M. Wieruzeski, P. Talaga, J.P. Bohin, and H. Desvaux, *J. Am. Chem. Soc.*, 118 (1996) 7227–7228.
[26] P. Berthault, N. Bilirakis, G. Rubinstenn, P. Sinay, and H. Desvaux, *J. Biomol. NMR*, 8 (1996) 23–35.
[27] D. Neuhaus and M.P. Williamson, *The Nuclear Overhauser effect in structural and conformational analysis*, VCH, New York, 1989.
[28] G. Esposito and A. Pastore, *J. Magn. Res.*, 76 (1988) 331–336, and references therein.
[29] D.J. Craik, A. Kumar, and G.C. Levy, *J. Chem. Inf. Comput. Chem.*, 23 (1983) 30–38.
[30] D.G. Davis, *J. Am. Chem. Soc.*, 109 (1987) 6962.
[31] H. van Halbeek and L. Poppe, *Magn. Res. Chem.*, 30 (1992) S74–S86.
[32] P.J. Hajduk, D.A. Horita, and L. Lerner, *J. Am. Chem. Soc.*, 115 (1993) 9196–9201.
[33] F. Heatley, *Prog. NMR Spectrosc.*, 13 (1979) 47.
[34] G. Wagner, *Curr. Opin. Struct. Biol.*, 3 (1993) 748–754.
[35] (a) P. Dais, *Carbohydr. Res.*, 263 (1994) 13–24; (b) L. Poppe, H. van Halbeek, D. Acquotti, and S. Sonnino, *Biophys. J.*, 66 (1994) 1642–1652; (c) S.B. Engelsen, C. Herve du Penhoat, and S. Perez, *J. Phys. Chem.*, 99 (1995) 13,334–13,351.
[36] M. Hricovini, M. Guerrini, G. Torri, and B. Casu, *Carbohydr. Res.*, 300 (1997) 69–76.
[37] J.R. Brisson, S. Uhrinova, R.J. Woods, M. van der Zwan, H.C. Jarrell, L.C. Paoletti, D.L. Kasper, and H.J. Jennings, *Biochemistry*, 36 (1997) 3278–3292.
[38] Q. Xu and C.A. Bush, *Biochemistry*, 35 (1996) 14,512–14,520.